Supporting Information

Baboolal et al. 10.1073/pnas.0909851106

SI Text

Construction of the Chimeric Myo5–2IQ-SAH Molecular Model. Construction of the chimeric Myo5 model (Fig. 1) was made by using Swiss-PdbViewer (1) and PyMOL (DeLano Scientific). A coiled-coil model (newsmbeam.pdb, G. Offer), 175 residues long, was aligned to the Cα backbone coiled coil of a scallop myosin model (2). To the head-tail junction of the scallop myosin model, an α-helical model of MyoM residues 931-1042 (i.e., the entire SAH domain), which also included the sequence of the final (6th) IQ domain of Myo5 was aligned to create the extension of the coiled coil. Backbone atoms of this IQ were then aligned to the second IQ motif of the Apo CaM/IQ crystal structure of Myo5 (2IX7.pdb), which contains two IQ motifs: IQ1 and IQ2 (3). The first IQ motif of 2IX7 was then aligned to the IQ motif of the crystal structure of Apo Myo5 motor with bound essential light chain (1OE9.pdb) (4).

Optical Trap Methods. An assay chamber, with a volume of approximately 30 μL, was constructed by using a coverslip decorated sparsely with 1.9-μm diameter glass microspheres (Bangs Laboratories) and a microscope slide attached using double-sided adhesive tape (5, 6). The Myo5–2IQ-SAH chimera was diluted to a concentration of approximately 0.01–0.03 mg·mL^{-1} in a buffered salt solution (AB$^-$) containing 25 mM KCl, 25 mM imidazole, 4 mM $MgCl_2$, and 1 mM EGTA; pH 7.4 at 22 °C (7) and allowed to bind inside the prepared chamber. To reduce any unspecific binding of the actin filament and beads to the surface of the chamber, approximately four chamber volumes of AB$^-$ containing 1 mg·mL^{-1} BSA (AB$^-$/BSA) was flushed through the chamber. Finally, AB$^-$/BSA was replaced using a solution based on AB$^-$ supplemented by the following reagents: 2 mM creatine phosphate, 50 mM DTT, 500 nM ATP, 0.1 mg·mL^{-1} creatine kinase, 3 mg·mL^{-1} glucose, 0.1 mg·mL^{-1} glucose oxidase and 0.02 mg·mL^{-1} catalase (8). In addition, the solution included 2 μM *Xenopus* calmodulin, 0.2 nM rhodamine-phalloidin (Invitrogen, Corp.) labeled, 10% biotinylated filamentous actin and NeutrAvidin (Thermo Fisher Scientific) coated 1-μm biotin-labeled polystyrene beads (5, 9). To visualize both the actin filament and the 1-μm polystyrene beads simultaneously using fluorescence illumination, the beads were treated with BSA conjugated with tetramethylrhodamine B-isothiocyanate (TRITC-BSA). A single actin filament was attached to two 1-μm NeutrAvidin-biotinylated polystyrene beads, separated by approximately 5–7 μm, via manipulation of the optical tweezers to form a "dumbbell." The dumbbell was made taut and was positioned above the third silica bead (i.e., pedestal) to record unitary acto-myo5–2IQ-SAH chimera interactions occasionally. Only one out of 10 pedestals exhibited unitary acto-myo5–2IQ-SAH chimera interactions. Experiments were performed with an optical trap stiffness between 0.015 and 0.03 pN·nm^{-1}.

The displacements of the two polystyrene beads were monitored by using optical magnification of the shadow of the beads projected onto a pair of quadrant photodiode detectors (10). Data were sampled at 10 kHz while sine waves (frequency = 200 Hz) of multiple amplitudes (100–300 nm, peak-to-peak) were applied to one or both of the optical tweezers (6, 11). Change in the amplitude of the sine-wave pickup was used to monitor the total system stiffness of the dumbbell system. Decrease in the standard deviation of the noise level of this sine wave was used as the criterion to distinguish regions of the collected data, either as periods with or without myosin attachments. Analysis was performed by using custom software written in IGOR Pro 6.0 (Wavemetrics, Inc.) and LabVIEW 6.0 (National Instruments, Corp.). Histograms were plotted by using SigmaPlot 9.0 (Systat Software, Inc.).

Transient Kinetics Methods. Stopped-flow measurements were done at 20 °C by using an SF-2001 stopped-flow apparatus (KinTek Corp.) fitted with two 2-mL and one 5-mL syringe. The excitation light from a 75-watt xenon lamp was selected by using a 0.2-m monochromator (Photon Technology International). Deac-aminoATP, was excited at 430 nm, and the emitted light was selected using a 450 nm long-pass filter. Stocks of Myo5–2IQ-SAH were diluted from buffer containing 400 mM KCl to obtain the desired protein concentration and a final KCl concentration of 180 mM just before use. In the double mixing experiments Myo5–2IQ-SAH (0.4 μM heads) and deac-aminoATP (0.5 μM) were mixed, aged in a delay line for 20 s to allow nucleotide binding and hydrolysis on both heads, and then mixed with actin solution containing an excess of ATP or ADP to prevent deac-aminoADP rebinding (also in buffer with no KCl). The final concentration of buffer in the flow cell was 10 mM Mops, pH 7.5, 3 mM $MgCl_2$, 40 mM KCl, 1 mM EGTA, and 1 mM DTT. Actin filaments were stabilized with equimolar phalloidin. Stock solutions of actin (80 μM) and ADP (2 mM) were treated for 1 h at 20 °C with 1 mM glucose and 0.01 unit·mL^{-1} hexokinase to remove traces of ATP in experiments where the actin contained an ADP chase. Stopped flow datasets containing 1,000 points were collected on a log time-base to avoid biasing the fitting toward slower processes. The data were initially fit using the fitting routines provided with the Kintek stopped-flow and were refit and plotted for publication using the nonlinear least squares routines in the Scientist package. Multiexponential data can be robustly fit to amplitudes and rate constants if the component rates differ by more than a factor of 5 but the data can be fit equally well by more than a single set of parameters if the rate constants differ by less than a factor of 4.

In these experiments, both heads of the Myo5–2IQ-SAH containing deac-aminoADP·P_i rapidly bind to actin. Comparing the rate(s) of ADP release using either an ATP or ADP chase shows whether the kinetics of the two heads are gated. If ADP releases first from the trail head and an ATP chase is used, this head would bind ATP and rapidly dissociate relieving any backward strain on the lead head which would then release its products at the same rate as that of the trail head. (The detached head becomes the new lead attached head faster than ADP is released, especially in the case of deac-aminoADP release, which is 10 times slower than ADP release). On the other hand if the ADP chase is used, the deac-aminoADP in the trail head would be quickly replaced by ADP, which keeps the trail head tightly bound to actin so it would continue to strain the lead head. In this case, if there is gating, a second slower exponential is seen in the transient that represents the gated release of ADP from the lead head and the amplitude of the fast phase is reduced.

1. Guex N, Peitsch MC (1997) SWISS-MODEL and the Swiss-PdbViewer: An environment for comparative protein modeling. *Electrophoresis* 18:2714–2723.
2. Offer G, Knight P (1996) The structure of the head-tail junction of the myosin molecule. *J Mol Biol* 256:407–416.

3. Houdusse A, et al. (2006) Crystal structure of apo-calmodulin bound to the first two IQ motifs of myosin V reveals essential recognition features. *Proc Natl Acad Sci USA* 103:19326–19331.
4. Coureux PD, et al. (2003) A structural state of the myosin V motor without bound nucleotide. *Nature* 425:419–423.
5. Takagi Y, Homsher EE, Goldman YE, Shuman H (2006) Force generation in single conventional actomyosin complexes under high dynamic load. *Biophys J* 90:1295–1307.
6. Veigel C, Bartoo ML, White DC, Sparrow JC, Molloy JE (1998) The stiffness of rabbit skeletal actomyosin cross-bridges determined with an optical tweezers transducer. *Biophys J* 75:1424–1438.
7. Kron SJ, Spudich JA (1986) Fluorescent actin filaments move on myosin fixed to a glass surface. *Proc Natl Acad Sci USA* 83:6272–6276.
8. Kishino A, Yanagida T (1988) Force measurements by micromanipulation of a single actin filament by glass needles. *Nature* 334:74–76.
9. Rock RS, Rief M, Mehta AD, Spudich JA (2000) In vitro assays of processive myosin motors. *Methods* 22:373–381.
10. Molloy JE, Burns JE, Kendrick-Jones J, Tregear RT, White DC (1995) Movement and force produced by a single myosin head. *Nature* 378:209–212.
11. Batters C, et al. (2004) Myo1c is designed for the adaptation response in the inner ear. *EMBO J* 23:1433–1440.

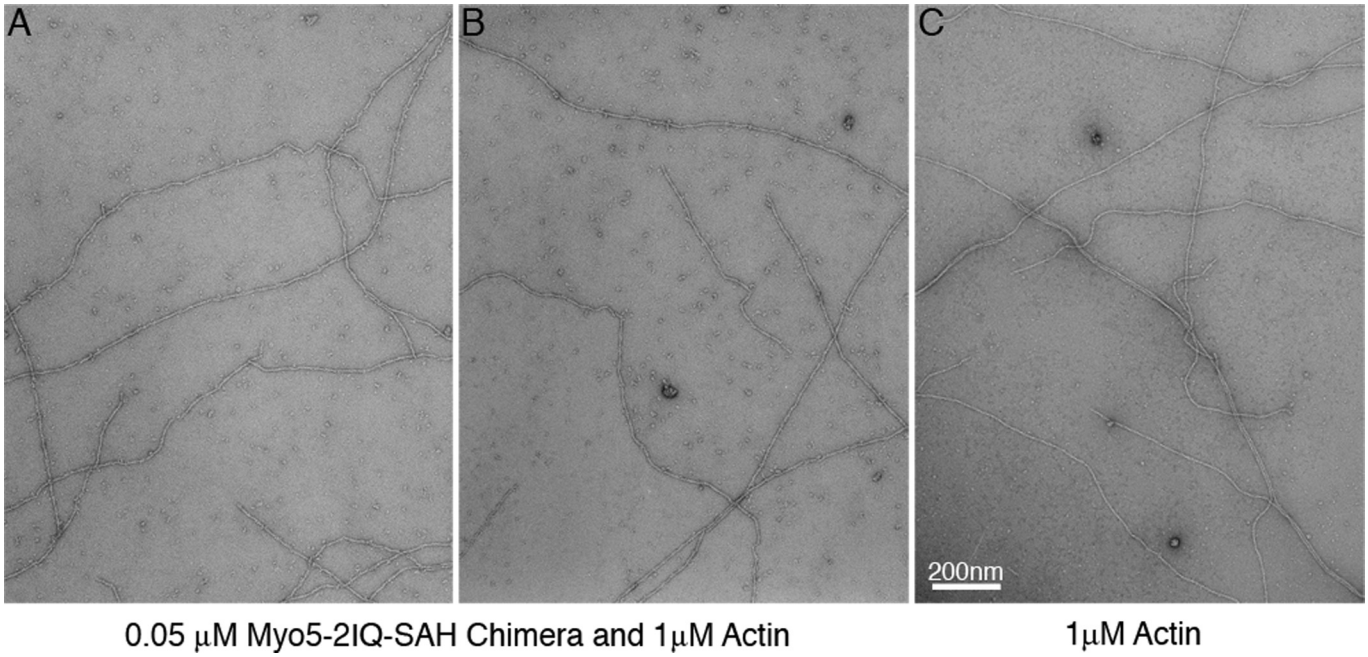

Fig. S1. Absence of actin bundling by Myo5–2IQ-SAH chimera during ATPase activity. (*A* and *B*) Representative electron micrographs of 1 μM F-actin mixed with 0.05 μM Myo5–2IQ-SAH chimera, and negative stained with 1% uranyl acetate. (*C*) A representative electron micrograph of F-actin in the absence of the chimera. The ratio of myosin to actin used here (1:20) is higher than that used in the ATPase assays (1:50), yet no bundling of the actin was observed. This indicates that binding of the two heads of the chimera to adjacent actin filaments does not occur in the ATPase assay, and that such binding cannot underlie the lack of gating in the chimera.